

# DECENTRALIZED CONTROL OF NANOSATELLITES SPATIAL DISTRIBUTION IN THE SWARM IN LEO USING MAGNETORQUERS

Danil Ivanov\*, Uliana Monakhova†, Dmitry Roldugin‡

The paper is devoted to the nanosatellites swarm control algorithms. The satellites in the swarm move along arbitrary relative trajectories according to the initial conditions after the launch. Each satellite is provided with the information about the relative motion of other satellites inside certain communication area. The purpose of the control is to achieve required spatial distribution of satellites in the along-track direction. The paper develops the corresponding decentralized control algorithm using the differential drag force. The required attitude control for each satellite is implemented by active magnetic attitude control system.

## INTRODUCTION

Swarm is a type of the satellite formation flight involving a considerable number of satellites that move along disordered relative trajectories. Swarm-type flight requires only bounded relative motion with no other restrictions. The advantage of random relative trajectories in the swarm is the economy of the control source of the satellites, less dependence on the failure of the specific satellite and reduced demands for the required onboard hardware and software. The swarm of satellites is able to construct the robust remote sensing system or to measure the spatial distribution of the near-Earth magnetosphere parameters at different scales. However, this requires specific control of spatial distribution of satellites in the swarm. The paper develops the corresponding decentralized control algorithm.

For the swarm of satellites in the Low-Earth-Orbit the most promising control approach is to use the aerodynamic forces. It does not require propellant, however, special form-factor satellites are required. Aerodynamic force acting on the satellite depends on its attitude. Attitude control is necessary to achieve the desirable relative motion. Magnetorquers are considered in this paper as the most suitable actuators for nano- and especially femto-satellites. Magnetic control systems are widely used for satellite angular velocity damping and attitude stabilization. They are by far the cheapest and are among the most reliable, small and lightweight. The drawbacks are the worst accuracy and under actuation. However, it is possible to achieve three axis stabilization using the magnetorquers. Proper stabilization requires the real-time determination of the attitude motion. It is obtained by processing the attitude sensors measurements. For example, the three axis attitude control is available with the sole magnetometer and three magnetorquers for a CubeSat.

---

\*Senior researcher, Space System Dynamics Department, Keldysh Institute of Applied Mathematics RAS, Miusskaya Sq.4, Moscow, Russia.

†Junior researcher, Space System Dynamics Department, Keldysh Institute of Applied Mathematics RAS, Miusskaya Sq.4, Moscow, Russia.

‡Senior researcher, Space System Dynamics Department, Keldysh Institute of Applied Mathematics RAS, Miusskaya Sq.4, Moscow, Russia.

Each satellite in the swarm requires the information about the relative motion of all other satellites for the control calculation. This is a difficult task for a large number of satellites in the swarm due to the hardware limitations of the relative motion determination system and/or the inter-satellite communication limitations. These restrictions are henceforth referred to as communicational constraints. Each satellite can estimate the relative motion of other satellites using the onboard motion determination system. However, due to the limited capabilities of the sensors, this is possible in a certain neighborhood only. These features of the autonomous motion determination system can be overcome by sharing information between satellites about the current orbital motion. However, inter-satellite communication channels also cannot provide unlimited number of connections to one satellite which is caused by the frequency restrictions. These communication constraints should be taken into account during the control of a swarm of satellites.

The control approach based on the differential drag force was firstly proposed in 1980s by Leonard <sup>1</sup> under the assumption of a discrete change in the effective cross section of satellites flying in the group. He developed a control algorithm based on the proportional differential controller. A large number of papers applied a big variety of the different control algorithms using differential drag: PID regulator <sup>2</sup>, linear-quadratic regulator <sup>3</sup>, Lyapunov-based control <sup>4,5</sup>, sliding mode control <sup>6</sup>, optimal control <sup>7</sup> etc. However, almost all the papers consider only two satellites in formation flying with application of the centralized control approach. A few papers are devoted to differential drag control of the multiple satellites. The cyclic and optimal control strategies for a cluster flight with more than two satellites are proposed in the paper <sup>8</sup>. Stability and performance of cluster keeping while avoiding collisions is studied in the <sup>9</sup>. The paper <sup>10</sup> of the authors of this work address communicational restrictions and decentralized control features for the swarm of nanosatellites deployment problem, though the attitude implementation issue was not considered.

The paper considers a swarm of 3U Cubesats in LEO. Initial conditions provide unbounded trajectories. Out-of-plane motion is fully determined by the initial conditions due to the fact that the differential drag is applied only in the along-track direction. Decentralized control is developed to prevent the relative drift and to achieve the required spatial distribution in the along-track direction. The relative trajectory projection on the orbital plane is the elliptical spiral. Therefore, the control of swarm distribution is related to the relative position of the instant center of the ellipses. A set of decentralized strategies to implement the calculated control taking into account the communicational constraints is considered. The performance of the proposed control strategies is studied numerically. The numerical simulation of the controlled relative motion of satellites in the swarm takes into account the second harmonic of the gravitational field and uncertainties in the atmospheric density. IGRF model is used for Earth magnetic field simulation. The CubeSat standard iron-core magnetorquers are considered for attitude control.

## **THE PROBLEM STATEMENT**

The problem of the satellite swarm construction after their separation from the launcher is considered, i.e. the achievement of closed relative trajectories is required. Each satellite is assumed to have its own spherical area of communication (see Figure 1). When a satellite enters this area of a neighboring satellite, its relative motion becomes known for that satellite. This information can be obtained either via an inter-satellite link or using autonomous relative motion determination system (range finders, optical sensors, etc).

At the initial time the satellites move in accordance with the specified initial conditions after deploying from the launcher. The satellites deployment is carried out using a certain launch system (usually by special springs) with a certain execution error. In the absence of control it leads to a gradual increasing distances between the satellites and the swarm degrades. Consider the swarm launched into LEO. Each satellite is assumed to be equipped with the attitude control

system, for example, reaction wheels-based one. So, the satellites are able to be controlled by the aerodynamic drag force which depends on the attitude of satellite relative to the incoming airflow. In the paper the 3U CubeSats are considered. They are the most popular nanosatellite nowadays and they have a form-factor quite proper for aerodynamic control because the ratio of the maximum to the minimum cross-sectional area is 3.

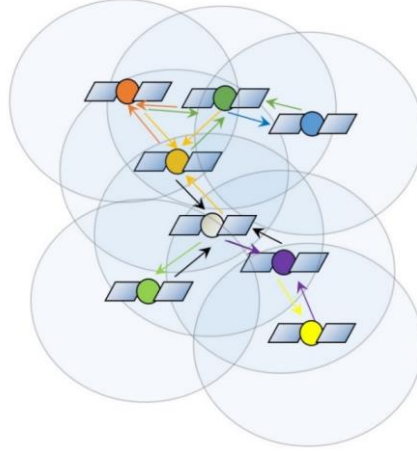


**Figure 1. Swarm of satellites with communication areas and communication links**

The main goal of the study is to develop such a decentralized control of satellites which leads the relative drift to zero for all satellites in the swarm. The possibility of constructing a swarm with piecewise constant control depending on initial conditions and communication constraints is investigated. The effect of these parameters on the integrity of the swarm during the implementation of differential drag control is considered too.

### Undisturbed Motion Equations

Consider a swarm of satellites moving along the close near circular orbits. It is convenient to use the motion equations written in the relative reference frame to describe the trajectories of satellites. The general form of the equations of the relative motion of two satellites is too complex for analytical consideration, so Hill-Clohessy-Wiltshire equations are used [22, 23]. The model describes the relative motion of two arbitrarily chosen satellites from a swarm in the central Newtonian gravitational field. The orbital reference frame is used, its origin (reference point) moves along a circular orbit of radius  $r_0$  with the orbital angular velocity  $\omega = \sqrt{\mu/r_0^3}$  where  $\mu$  is the Earth gravitational parameter. Axis  $Oz$  is aligned with the vector from the center of the Earth to the reference point, axis  $Oy$  is directed along the normal to the orbital plane, axis  $Ox$  complements the reference frame to the right-handed one (Fig. 2).

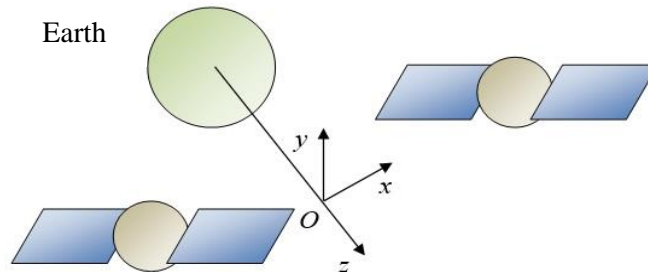


**Figure 2. The reference frame associated with the  $O$  reference point moving in a circular orbit**

Let  $\mathbf{r}_i = (x_i, y_i, z_i)$  and  $\mathbf{r}_j = (x_j, y_j, z_j)$  be the vectors of the conditional  $i$ -th and  $j$ -th satellites in the reference frame,  $i \neq j$ ,  $i = 1, \dots, N$ ,  $j = 1, \dots, N$  where  $N$  is the number of the satellites in the swarm. Then the components of the relative position vector  $\mathbf{r}_{ij} = \mathbf{r}_j - \mathbf{r}_i = (x_{ij}, y_{ij}, z_{ij})$  in the case of free motion are governed by the following equations

$$\begin{aligned}\ddot{x}_{ij} + 2\omega\dot{z}_{ij} &= 0, \\ \ddot{y}_{ij} + \omega^2 y_{ij} &= 0, \\ \ddot{z}_{ij} - 2\omega\dot{x}_{ij} - 3\omega^2 z_{ij} &= 0,\end{aligned}\tag{1}$$

The solution of the equations is as follows:

$$\begin{aligned}x_{ij}(t) &= -3C_1^{ij}\omega t + 2C_2^{ij}\cos(\omega t) - 2C_3^{ij}\sin(\omega t) + C_4^{ij}, \\ y_{ij}(t) &= C_5^{ij}\sin(\omega t) + C_6^{ij}\cos(\omega t), \\ z_{ij}(t) &= 2C_1^{ij} + C_2^{ij}\sin(\omega t) + C_3^{ij}\cos(\omega t),\end{aligned}$$

where  $C_1^{ij} - C_6^{ij}$  are constants that depend on the initial conditions at  $t = 0$ :

$$\begin{aligned}C_1^{ij} &= \frac{\dot{x}_{ij}(0)}{\omega} + 2z_{ij}(0), C_2^{ij} = \frac{\dot{z}_{ij}(0)}{\omega}, C_3^{ij} = -3z_{ij}(0) - \frac{2\dot{x}_{ij}(0)}{\omega}, \\ C_4^{ij} &= x_{ij}(0) - \frac{2\dot{z}_{ij}(0)}{\omega}, C_5^{ij} = \frac{\dot{y}_{ij}(0)}{\omega}, C_6^{ij} = y_{ij}(0).\end{aligned}\tag{2}$$

The term responsible for the relative drift is  $-3C_1^{ij}\omega t$ . Thus, the relative trajectory of two satellites is closed if and only if  $C_1^{ij} = 0$ . However, in practice such an ideal initial conditions for free motion cannot be specified, and in the case of perturbations and nonlinear effects there is always a relative drift between the satellites. Therefore, the satellites must be controlled to eliminate the drift and to achieve the bounded relative trajectory.

In the case of a swarm it is required to consider the pairwise relative motion between all satellites. For bounded relative trajectories of all satellites in the swarm each  $C_1^{ij}$  must converge to zero. So, the problem of the swarm construction after the launch is to eliminate all relative drifts.

### Controlled Motion Equations

Consider the application of the aerodynamic drag force for the swarm control. Since the drag force is directed against the satellite velocity vector and the swarm moves in near circular orbit it is assumed that the drag force is aligned with  $Ox$  axis. The model of aerodynamic drag force  $f_i$  acting on the  $i$ -th satellite can be represented in the following form:

$$f_i = -\frac{1}{2}C_a\rho V^2\Delta S \sin\alpha_i - \frac{1}{2}C_a\rho V^2 S_0\tag{3}$$

where  $C_a$  is the aerodynamic drag coefficient,  $\rho$  is the density of the atmosphere,  $V$  is the velocity of the incoming flow,  $\Delta S$  is the difference between maximum and minimum value of the cross-sectional area of satellite,  $S_0$  is the minimum value of the cross-sectional area of satellite,  $\alpha_i \in [0; \pi/2]$  is the angle between the direction of the incoming airflow and longitudinal axis of satellites that is assumed to be axisymmetric. The satellites are supposed to be identical, so the values of the  $\Delta S$ ,  $S_0$ ,  $C_a$  are the same for all satellites. The velocity of the atmosphere due to the Earth rotation is neglected and the velocity of the incoming flow for all

satellites is assumed to be equal to the orbital velocity  $V = \sqrt{\mu / r_0}$ . The satellites are equipped with attitude control system, it allows them to change the angle  $\alpha$  and thereby to control the value of the aerodynamic drag force.

The difference between aerodynamic drag forces acting on the  $i$ -th and  $j$ -th satellites taking into account that the second term is equal for all satellites is as following:

$$f_{ij} = f_j - f_i = -\frac{1}{2} C_a \rho V^2 \Delta S (\sin \alpha_j - \sin \alpha_i). \quad (4)$$

According to the differential drag model the force value is limited and the maximum value is

$$\max |f_{ij}| = \frac{1}{2} C_a \rho V^2 \Delta S.$$

Consider controlled motion equations of a swarm. Since the control is implemented using differential drag force the acceleration vector  $\mathbf{u}_{ij} = \mathbf{u}_j - \mathbf{u}_i = (u_x^{ij}, u_y^{ij}, u_z^{ij})$  has a non-zero component along the  $Ox$  axis only, i.e.  $u_y^{ij} = u_z^{ij} = 0$ . Let  $u_{ij} = u_x^{ij} = f_{ij} / m$  where  $m$  is the mass of the satellite. Then the relative motion equations for  $i$ -th and  $j$ -th satellites are as follows:

$$\begin{aligned} \ddot{x}_{ij} + 2\omega \dot{z}_{ij} &= u_{ij}, \\ \ddot{y}_{ij} + \omega^2 y_{ij} &= 0, \\ \ddot{z}_{ij} - 2\omega \dot{x}_{ij} - 3\omega^2 z_{ij} &= 0. \end{aligned}$$

The differential aerodynamic drag force has no effect on the motion along  $Oy$  axis, it is defined only by the initial conditions after the launch. That is why a planar motion of the satellites in  $Oxz$  plane is considered in the paper.

### Angular Motion Equations

Rigid spacecraft angular motion is considered. The satellite is equipped with three mutually orthogonal magnetorquers and three axis magnetometer. Magnetorquers can produce any restricted dipole moment. Disturbing torques include gravitational and unknown ones. The latter are represented by constant and/or arbitrary Gaussian values. Inertia tensor knowledge is also erroneous.

Satellite attitude is represented using Euler angles  $\alpha, \beta, \gamma$  (rotation sequence 2-3-1), direction cosines matrix  $\mathbf{A}$  and its elements  $a_{ij}$  (used for analytical study) and quaternion  $\Lambda = (\mathbf{q}, q_0)$  (used for numerical simulation). Angular velocity may represent either absolute motion ( $\boldsymbol{\omega}$  and its components  $\omega_i$ ) or relative motion with respect to orbital reference frame ( $\boldsymbol{\Omega}$  and  $\Omega_i$ ). Absolute and relative velocities are related by

$$\boldsymbol{\omega} = \boldsymbol{\Omega} + \mathbf{A} \boldsymbol{\omega}_{orb} \quad (5)$$

where  $\boldsymbol{\omega}_{orb} = (0, \omega_0, 0)$  is the orbital reference frame angular velocity.

Euler equations for the satellite with arbitrary inertia tensor  $\mathbf{J} = \text{diag}(A, B, C)$  are

$$\mathbf{J} \dot{\boldsymbol{\omega}} + \boldsymbol{\omega} \times \mathbf{J} \boldsymbol{\omega} = \mathbf{M} \quad (6)$$

for absolute angular velocity and

$$\mathbf{J} \dot{\boldsymbol{\Omega}} + \boldsymbol{\Omega} \times \mathbf{J} \boldsymbol{\Omega} = \mathbf{M} + \mathbf{M}_{rel} \quad (7)$$

where  $\mathbf{M}_{rel} = -\mathbf{J}\mathbf{W}_\omega\mathbf{A}\boldsymbol{\omega}_{orb} - \boldsymbol{\Omega} \times \mathbf{J}\mathbf{A}\boldsymbol{\omega}_{orb} - \mathbf{A}\boldsymbol{\omega}_{orb} \times \mathbf{J}(\boldsymbol{\Omega} + \mathbf{A}\boldsymbol{\omega}_{orb})$  for relative angular velocity.  $\mathbf{W}_y$  is a skew-symmetric matrix for any  $\mathbf{y}$ ,

$$\mathbf{W}_y = \begin{pmatrix} 0 & y_3 & -y_2 \\ -y_3 & 0 & y_1 \\ y_2 & -y_1 & 0 \end{pmatrix}. \quad (8)$$

The torque may contain control part  $\mathbf{M}_{ctrl}$  and disturbing part. The latter is divided into gravitational and unknown one,  $\mathbf{M} = \mathbf{M}_{ctrl} + \mathbf{M}_{gr} + \mathbf{M}_{dist}$ .

Dynamical equations are supplemented with kinematic relations. Quaternion kinematics is

$$\begin{aligned} \dot{\mathbf{q}} &= \frac{1}{2}(q_0\boldsymbol{\Omega} + \mathbf{W}_\Omega\mathbf{q}), \\ \dot{q}_0 &= -\frac{1}{2}\mathbf{q}^T\boldsymbol{\Omega}. \end{aligned} \quad (9)$$

Control torque is  $\mathbf{M}_{ctrl} = \mathbf{m} \times \mathbf{B}$  where  $\mathbf{m}$  is the dipole control moment of the satellite,  $\mathbf{B}$  is the geomagnetic induction vector in bound reference frame. Consider control torque based on the PD-controller

$$\mathbf{m} = -k_\omega\mathbf{B} \times \boldsymbol{\Omega} - k_a\mathbf{B} \times \mathbf{S} \quad (10)$$

where  $\mathbf{S} = (a_{23} - a_{32}, a_{31} - a_{13}, a_{12} - a_{21})^T$ . It provides necessary attitude<sup>13-15</sup>. Control parameters have decisive influence on the algorithm performance. They are adjusted manually in the vicinity of optimal ones obtained using Floquet theory<sup>16</sup>.

Gravitational torque is

$$\mathbf{M}_{gr} = 3\omega_0^2(\mathbf{A}\mathbf{e}_3) \times \mathbf{J}(\mathbf{A}\mathbf{e}_3) \quad (11)$$

where  $\mathbf{e}_3 = (0, 0, 1)$  is the satellite radius-vector in orbital frame.

Unknown disturbing torque is modelled using three different approaches. Gaussian distribution of the order of  $5 \cdot 10^{-7} N \cdot m$  allows modelling arbitrary disturbances with small effect on satellite motion since control torque is few orders greater. Constant disturbance on the level of  $10^{-7} N \cdot m$  augmented with Gaussian one represents more notable disturbance. Constant torque may arise due to aerodynamics or solar pressure acting on a satellite with vast solar panels. The worst case is constant torque of  $5 \cdot 10^{-7} N \cdot m$  value.

## LYAPUNOV CONTROL ALGORITHM

The main goal of control to form and maintain a swarm of satellites, that is, to eliminate relative drift and limit relative trajectories. The shape and size of relative trajectories is determined by constants  $C^{ij}$  in order for the swarm to be in a certain area, we will manage the position of the centers of instantaneous ellipsoids, which are in general trajectories of relative motion. From the equations of motion (1) one can conclude that the constants  $C_1^{ij}$  are responsible for eliminating the drift, and the constants  $C_4^{ij}$  are responsible for the position of the center of the instantaneous ellipsoid of the trajectory. So, the goal of control is to hold the values  $C_4^{ij}$  less than a certain reference values  $\tilde{C}_4^{ij}$  and eliminate the relative drift  $C_1^{ij}$ . For developing such a control consider the Lyapunov candidate function:

$$V = \frac{1}{2}(C_1^{ij})^2 + \frac{1}{2}(\Delta C_4^{ij})^2, \quad (12)$$

Where  $\Delta C_4^{ij}$  is the difference between  $\tilde{C}_4^{ij}$  and real value  $C_4^{ij}$ . It is easy to verify that for (19) the conditions  $V > 0$ ,  $V(0) = 0$  are satisfied. Let's demand that the derivative of the Lyapunov function is negative  $\dot{V} < 0$ . The derivative is as follows:

$$\dot{V} = C_1^{ij} \dot{C}_1^{ij} + \Delta C_4^{ij} \Delta \dot{C}_4^{ij} = C_1^{ij} \left( \frac{\dot{x}^{ij}}{\omega} + 2\dot{z}^{ij} \right) + \Delta C_4^{ij} \left( \dot{x}^{ij} - \frac{2\dot{z}^{ij}}{\omega} \right).$$

Substitute  $\ddot{z}$  from (1) and obtain following control law:

$$\begin{aligned} \dot{V} &= \frac{1}{\omega} C_1^{ij} (\dot{x}^{ij} + 2\omega \dot{z}^{ij}) + \Delta C_4^{ij} \left( \dot{x}^{ij} - \frac{2}{\omega} (2\omega \dot{x}^{ij} + 3\omega^2 z^{ij}) \right) = \frac{1}{\omega} C_1^{ij} u_x + \Delta C_4^{ij} (-3\omega C_1^{ij}) \\ u^{ij} &= -k C_1^{ij} + 3\omega^2 \Delta C_4^{ij}, \quad k > 0. \end{aligned} \quad (13)$$

Thus, in the case of two i-th and j-th satellites, the control  $u_{ij}$  leads to a closed relative trajectory lying in a certain area defined by the value  $\tilde{C}_4^{ij}$ . Consider an implementation of this algorithm allows to achieve  $C_1^{ij} = 0$  and  $C_4^{ij} = \tilde{C}_4^{ij}$  for all the satellites in the swarm. One can not strive to achieve  $C_4^{ij} = \tilde{C}_4^{ij}$  for each device in each moment, but to control using only the average value  $\bar{C}_4^{ij}$  among the satellites within the communication sphere. For the i-th satellite with the number of satellites  $N_{comm}$ , the relative motion of which is known, the average  $\bar{C}_4^i$  is determined as follows:

$$\bar{C}_4^i = \sum_{j=1}^{N_{comm}} C_4^{ij} / N_{comm}.$$

The corresponding control applied to the satellite during the interval  $\Delta T$ , if its value  $\bar{C}_4^i$  is more than the reference value  $\tilde{C}_4^{ij}$ , according to (13) has the form:

$$u_i^{\bar{C}_4^i} = -k \bar{C}_1^i + 3\omega^2 \Delta \bar{C}_4^i \quad (14)$$

The final control scheme with regard to the implementation of the required angular motion using a magnetic attitude control system is shown in Fig. 3. Initially, the initial conditions for the integration of the equations of relative motion and the equations of angular motion for both satellites are determined. Then, using the current state vector, the relative drift and relative  $C_4^{ij}$  is calculated and using (14) the required control value is obtained. This value of aerodynamic force can be achieved if a certain attitude of both satellites is realized. Using the model of aerodynamic force (2), the required angles of orientation of the apparatus relative to the incident flow are calculated. After that, the magnetic control is aimed at stabilizing the satellite relative to the desired position. During stabilization, the actual position of the apparatus is used to calculate the aerodynamic force acting on it and to integrate the equations of relative motion. Updating the required control value to eliminate relative drift occurs at a certain time interval.

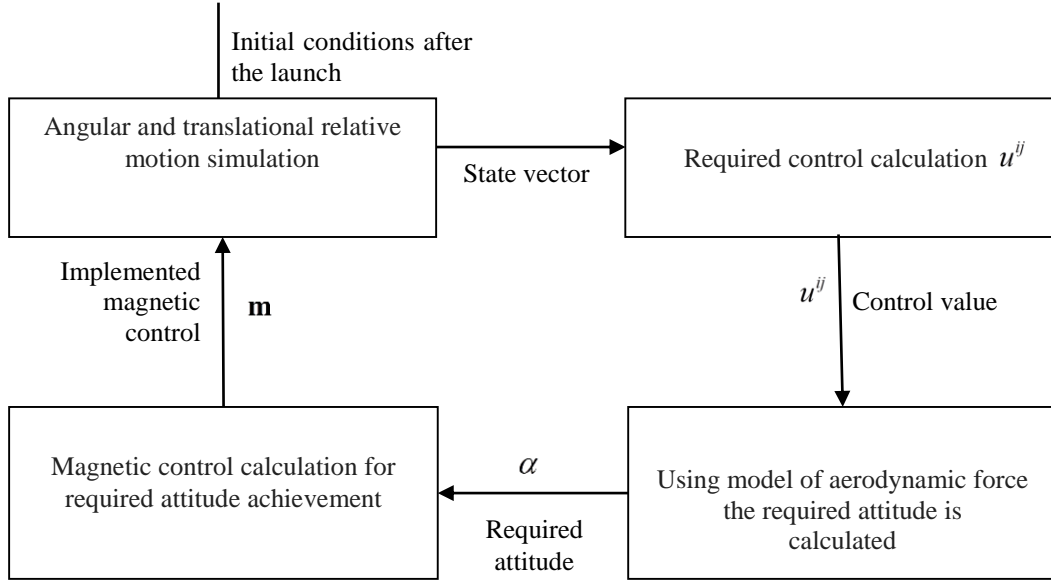


Figure 3. Control scheme

### Decentralized control approach

The decentralized control approach means that each satellite is controlled individually and independently based on the relative motion information. It is assumed that the calculated control applied to the other satellites could be unknown.

Since in the decentralized scheme each satellite is controlled independently then  $i$ -th satellite can just partly implement the calculated value  $u_{ij} = u_j - u_i$ . Value  $u_j$  cannot be known by  $i$ -th satellite then it can be considered as a disturbance in control for  $i$ -th satellite. According to the aerodynamic drag model  $u_i \in [-u_{\min}; -u_{\max}]$  where  $u_{\max} > 0$  is the absolute maximum value of the acceleration,  $u_{\min} > 0$  is the absolute minimum value of the acceleration. Thus, for the  $u_i$  one can derive the following decentralized control law:

$$u_i = \begin{cases} -u_{\max}, & \text{if } u_{ij} > (u_{\max} - u_{\min}), \\ -u_{ij} - u_{\min}, & \text{if } 0 < u_{ij} < (u_{\max} - u_{\min}), \\ -u_{\min}, & \text{if } u_{ij} < 0. \end{cases} \quad (15)$$

In the case of only two  $i$ -th and  $j$ -th satellites the applied control law (15) is the same but for the control value that is of different sign  $u_{ji} = -u_{ij}$ . If  $u_{ij} < 0$  then the value  $u_j$  obtained from (15) with  $u_{ji} > 0$  provides the calculated in (13) control, and the relative drift is eliminated. However, the simple control law (15) becomes unclear in case when it is required to achieve  $C_1^{ij} = 0$  for all the satellites in the swarm. Taking into account the communication restriction on the size of the communication area, control rules utilizing (13) is developed.

### Disturbances, uncertainties and collision avoidance

Low near circular Earth orbits experience three main sources of perturbations affecting the relative motion of satellites in the formation flying. Namely, these are the  $J_2$  second harmonic and slight oblateness of the orbits. However control errors caused by the inaccurate knowledge of the density of the atmosphere provide the most significant disturbance. The density of the

atmosphere in LEO can vary by several times along the circular orbit. It depends on the illumination and hence on the Sun activity. Atmospheric density models always have some errors. Moreover, the most accurate models may be hard to calculate on a possibly slow on-board computer. So the motion of two satellites is investigated in the case when the control algorithm is constructed using the linear model (1) with constant atmospheric density. The simulated motion however takes into account the orbit eccentricity, the second harmonic  $J_2$ , and the GOST atmosphere model of the upper Earth atmospheric density <sup>17</sup>.

Moreover, in this section the collision avoidance issue is also addressed. Since the satellites in the swarm are flying in random relative trajectories the collisions between them are possible. Consider a certain spherical vicinity around each satellite. If the satellite trajectory gets into this “dangerous” area the control algorithm switches from the swarm deployment to collision avoidance one. The purpose of the collision avoidance control can be formulated as follows: the satellite needs to leave the dangerous area as soon as possible or at least to enlarge the nearest relative distance <sup>10</sup>.

Consider the simulation parameters used for the example with the linear model. Orbital motion of each satellite is calculated in the inertial reference frame. Relative motion is obtained as a difference of positions and velocities in the orbital reference frame. The equations of motion in the inertial reference frame are

$$\begin{aligned}\ddot{\mathbf{R}}_i &= -\frac{\mu}{R_i^3} \mathbf{R}_i + \mathbf{D}_i^{J_2} + \mathbf{F}_i^a, \\ \mathbf{D}_i^{J_2} &= \frac{\delta}{R_i^5} \left( \frac{5Z_i^2}{R_i^2} - 1 \right) \mathbf{R}_i - 2 \frac{\delta}{R_i^5} \mathbf{Z}_i.\end{aligned}\tag{16}$$

Here  $\mathbf{R}_i = [X_i, Y_i, Z_i]$  is the radius vector of the  $i$ -th satellite in the inertial reference frame,  $\mathbf{D}_i^{J_2}$  is the disturbance vector caused by  $J_2$ ,  $\delta = 3J_2\mu R_E^2 / 2$ ,  $J_2 = 1082.6 \cdot 10^{-6}$ ,  $R_E = 6.378 \cdot 10^6$  m is the mean radius of the Earth,  $\mathbf{F}_i^a$  is the aerodynamic force in the inertial reference frame acting on the  $i$ -th satellite. The aerodynamic force is calculated by (3) where all vectors are expressed in the inertial reference frame. The density of the atmosphere is considered variable in accordance with the GOST model. The relative position  $\mathbf{r}_{ij}$  and relative velocity  $\mathbf{v}_{ij}$  of two satellites in the orbital reference frame are calculated using following formulas

$$\begin{aligned}\mathbf{r}_{ij} &= G(\mathbf{R}_j - \mathbf{R}_i), \\ \mathbf{v}_{ij} &= G\left[\left(\dot{\mathbf{R}}_j - \dot{\mathbf{R}}_i\right) + \boldsymbol{\omega} \times (\mathbf{R}_j - \mathbf{R}_i)\right],\end{aligned}\tag{17}$$

where  $G$  is the transition matrix from the inertial to the orbital reference frame,  $\boldsymbol{\omega}$  is the vector of the orbital angular velocity in the inertial reference frame.

GOST model requires the simulation start time, the level of solar activity  $F_0$ , the average daily solar activity index, the planetary average daily indices of the geomagnetic disturbance, and other parameters of the model. Let the start date be January 1, 2012, 0:00 AM. This defines all parameters of the model. In particular,  $F_0 = 125 \cdot 10^{-2}$  W / (m<sup>2</sup> · Hz) which characterizes the average level of the solar activity.

The inclination of the orbit  $i = 51.7^\circ$ . First satellite initial conditions are set such that it would move in a circular orbit in the central gravitational field. Namely, the velocity

$\dot{\mathbf{R}}_1(t_0) = \sqrt{\mu / (R_E + h)}$  is set perpendicular to the radius vector. Second satellite initial conditions are in accordance with constants (2). Position and velocity vectors of the second satellite in the orbital reference frame are

$$\mathbf{r}_{1j}(t_0) = \begin{bmatrix} 2C_2^{1j} + C_4^{1j} \\ C_6^{1j} \\ 2C_1^{1j} + C_3^{1j} \end{bmatrix}, \quad \mathbf{v}_{1j}(t_0) = \begin{bmatrix} -3C_1^{1j}\omega - 2C_3^{1j}\omega \\ \omega C_5^{1j} \\ 2C_2^{1j}\omega \end{bmatrix}$$

Position and velocity vectors in the inertial reference frame are

$$\begin{aligned} \mathbf{R}_j(t_0) &= \mathbf{R}_1(t_0) + G^T \mathbf{r}_{1j}(t_0), \\ \dot{\mathbf{R}}_j(t_0) &= \dot{\mathbf{R}}_1(t_0) + G^T \mathbf{v}_{1j}(t_0) + \boldsymbol{\omega} \times (G^T \mathbf{r}_{1j}(t_0)). \end{aligned}$$

Inertial trajectories are obtained with fourth-order Runge-Kutta integration. They are transformed into the relative ones according to (2). The resulting values are considered as the input to the control algorithm.

## NUMERICAL STUDY

Consider the application of the proposed control rules for the problem of the nanosatellites swarm construction after the launch. The scheme of the launch of the satellites is the same that was used by the PlanetLabs Company in 2017 to deploy 88 3U CubeSats<sup>18</sup>(Fig. 4). It is assumed that the satellites separate from the launcher in the  $Ox$  axis direction one after another with the time interval  $\Delta t$  between the ejections. The velocity of the ejection  $V_e$  is assumed to be the same for all CubeSats, however due to launch system inaccuracy the ejection velocity  $V_e$  is subjected to errors. So, the initial velocity vector  $\mathbf{V}_0$  in orbital reference frame is modelled as follows:

$$\mathbf{V}_0 = \begin{bmatrix} V_e + \delta V \\ \delta V \\ \delta V \end{bmatrix} \quad (18)$$

where  $\delta V$  is ejection error considered as normally distributed random value with zero mean and covariance  $\sigma_{\delta V}^2$ .



**Figure 4.** The screenshot of the video of the launch of the PlanetLabs 3U CubeSats<sup>18</sup>

All parameters used in the simulation of the controlled motion of the CubeSats swarm are presented in Table 1. In this section the constant atmosphere density model is used. The value of the density is chosen as an average atmosphere density along the orbit with 340 km altitude according to the Russian GOST Model of the Upper Atmosphere<sup>17</sup>.

**Table 1. Parameters of simulation**

Main parameters of the swarm

Number of satellites in the swarm, $N$	10
Time interval between control calculation, $\Delta T$	1500 s
Ejection parameters	
Time interval between the ejections, $\Delta t$	10 s
Ejection velocity, $V_e$	0.5 m/s
Ejection error deviation, $\sigma_{\delta V}$	0.015 m/s
CubeSats parameters	
Mass of satellite, $m$	3 kg
Difference between maximum and minimum value of the cross-sectional area, $\Delta S$	0.02 m <sup>2</sup>
Aerodynamic drag coefficient, $C_a$	2
Aerodynamic drag force parameters	
Constant atmosphere density, $\rho$	10 <sup>-11</sup> kg/m <sup>3</sup>
Orbit altitude, $h$	340 km
Airflow velocity, $V = \sqrt{\mu / (R_E + h)}$	7.69 km/s
Maximum of the control source, $u_{\max}$	4.1 · 10 <sup>-6</sup> m/s <sup>2</sup>
Minimum of the control source, $u_{\min}$	1.4 · 10 <sup>-6</sup> m/s <sup>2</sup>

**“Center” configuration**

Apply to the swarm of satellites the proposed decentralized control and select a value  $\tilde{C}_4^{ij} = 0$ . Thus, all mean values  $\bar{C}_4^i$  will tend to zero, which should bring all centers of relative trajectories to the origin. Control begins to be implemented immediately after all the satellites of the swarm are separated from the launch vehicle. The amount of control is calculated according to the formulas (14) depending on the value  $\bar{C}_4^i$  periodically in accordance with the time interval  $\Delta T = 150$  c. This control is implemented subject to the limitations of the aerodynamic drag force according to (2). The source of the reference was not found. In Fig. 5 and Fig. 6, the trajectories of relative motion are presented during the entire simulation time and on the last two turns, respectively. From the presented graphs it is clear that the trajectories gradually become close to closed and their centers come to the origin of reference frame. But due to disturbances, non-constant atmosphere density, collision avoidance control and control execution errors the trajectories seldom deviates its instant centers from the origin.

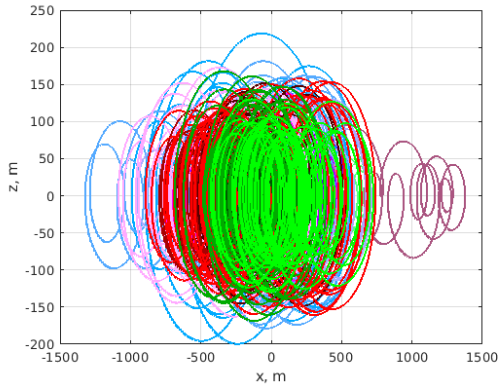


**Figure 5. Relative motion trajectories**

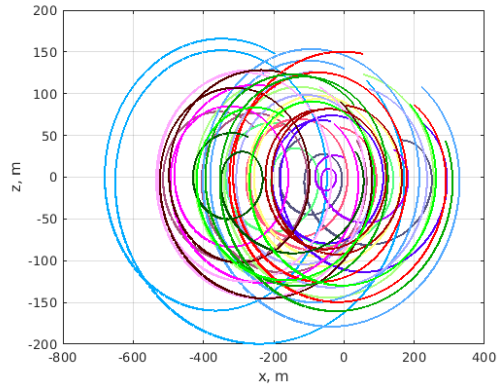


**Figure 6. Relative motion trajectories during the last two turns**

The change in values  $\bar{C}_4^i$  calculated at the time of implementation of the control, and the change in values  $C_4^{1j}$  that are proportional to the drift, calculated relative to the first launched vehicle, are presented in Fig. 7 and Fig. 8 respectively. Values  $\bar{C}_4^i$  and  $C_4^{1j}$  converge to zero, which again confirms that the relative trajectories of the satellites in the swarm become limited.

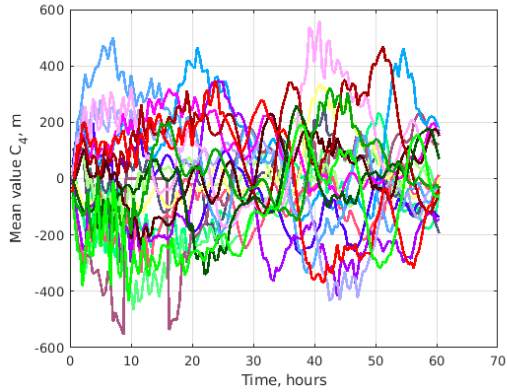


**Figure 7. Values of  $\bar{C}_4^i$  for all satellites**

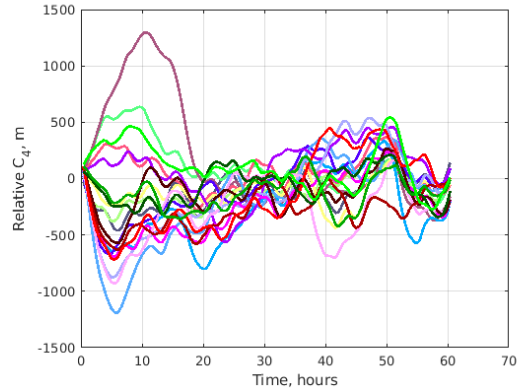


**Figure 8. Values  $C_4$  relative to the first launched satellite**

Fig. 9 shows the values of the required and actual attitude angle relative to the incident flow for one of the satellites in the swarm. The accuracy of the implementation of the required angles was about 20 degrees. Despite the low accuracy of the implementation of the required control, a swarm of satellites is being formed. Fig. 10 shows the values of the magnetic dipole moments of the coils during control.

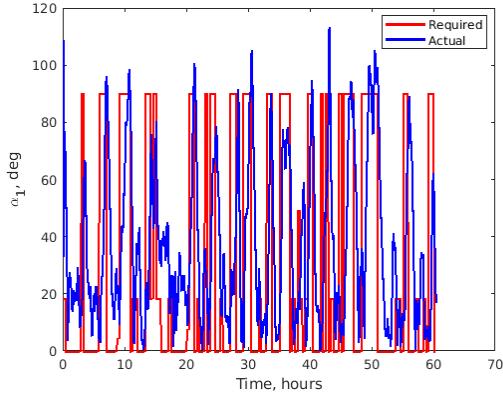


**Figure 9. Required and actual first satellite attitude**

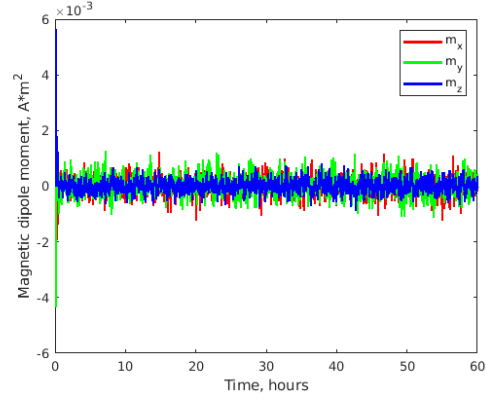


**Figure 10. Magnetic dipole moment**

Fig. 11 demonstrates the collision avoidance incidents, when the satellites come inside the dangerous spherical of area 10 m radius. In that case the control changes from the swarm construction to the repulsive one: one of the satellites tries to align its longitude axis along the incoming airflow when the other increase its cross-section area to maximize the relative distance during the close rendezvous. Fig. 11 shows when the satellite was in collision avoidance control mode and with which satellite. From Fig. 11 one can see that the satellites in collision avoidance mode are in pairs and in that very tight swarm it occurs rather often.

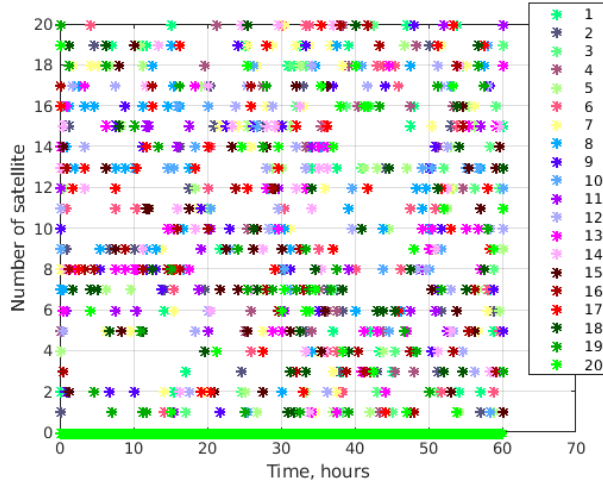


**Figure 11. Collision avoidance control**

### Motion in restricted area

Consider the proposed decentralized control only with a nonzero control value of  $\tilde{C}_4^{ij} = 300$  m. Thus, all average values  $\bar{C}_4^i$  will tend not to zero, but to values  $\bar{C}_4^i$  not exceeding 300 m. The control value is calculated according to (12) depending on the value  $\bar{C}_4^i$  periodically in accordance with the time interval  $\Delta T = 150$  c. This control is implemented taking into account the limitations of the aerodynamic drag force. Fig. 12 shows the trajectories of relative motion throughout the entire simulation time, and Fig. 13 shows the trajectories during last two orbital turns.

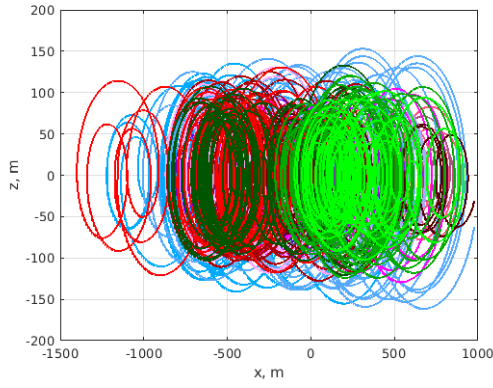


**Figure 12. Relative trajectories**

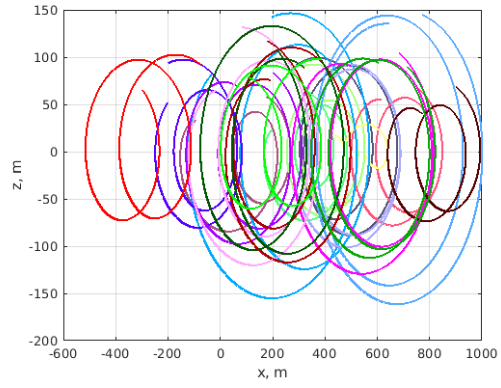


**Figure 13. Relative motion trajectories during the last two turns**

The change in the values  $\bar{C}_4^i$  calculated at the time of implementation of the control, and the change in the values  $C_4^{ij}$  calculated relative to the first launched satellite, are presented in Figure 14 and Figure 15, respectively. The values  $\bar{C}_4^i$  and  $C_4^{ij}$  at the time of the end of modeling do not go beyond the specified area, which again confirms that the relative trajectories of satellites in the swarm become limited.

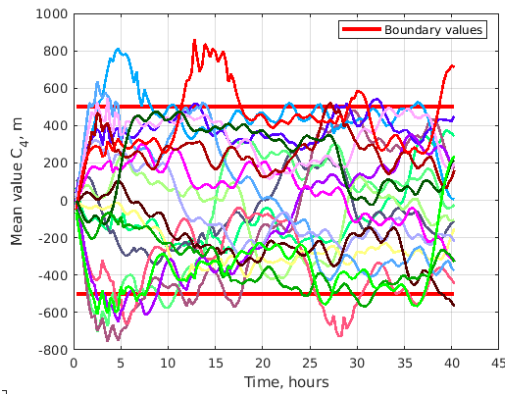


**Figure 14. Values  $\bar{C}_4^i$  for all satellites**

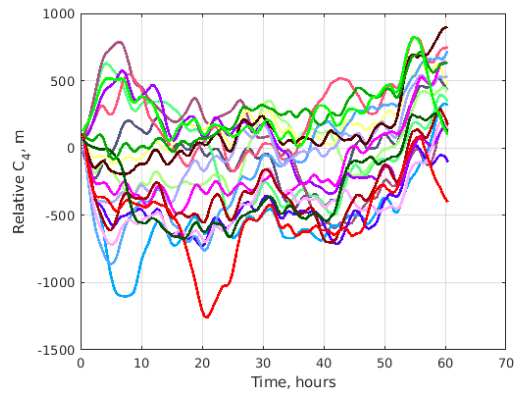


**Figure 15. Values  $C_4$  relative the first launched satellite**

The motion inside the specified area leads to not so tight swarm as for “center” configuration as one can see comparing Fig. 6 and 12. As a results the collision avoidance control is applied not so often comparing to the “center” configuration but the dangerous situations occurs periodically as one can see from Fig. 16.

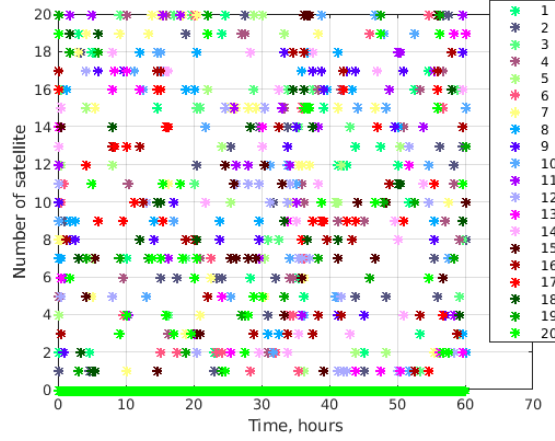


Figure 16. Collision avoidance control

### Uniform satellites distribution in along track direction

In the case the uniform relative position of the satellites in the swarm is required the satellites can be controlled in the terms of relative centers of instant elliptical trajectories, i.e. in terms of constants  $C_4$ . Consider a decentralized motion algorithm which aim is to achieve required constant  $\tilde{C}_4$  separation between the nearest neighbor satellites. The idea of the algorithm is in the following. Consider the  $i$ -th satellite with communication sphere. Inside this sphere the motion of all of the satellites is assumed to be known. Lets sort all the constants  $C_4$  for the  $i$ -th and find the nearest left-side satellite with smallest negative value  $\hat{C}_4^i$ . Then the difference between the x-coordinate of the instant center of the nearest left neighbor and the required centers separation  $\Delta C_4^i = \hat{C}_4^i - \tilde{C}_4$  will be used in the control law (13). In the case there is no left-side neighbor satellite the second term in (13) is equal to zero. In such a way the satellites in the swarm will align their relative  $C_4$  constants and the density of the satellites in the swarm become more uniform. However, since the control algorithm aim is not achieve the particular relative reference orbits the trajectories remains random in size and the phase, so the actual uniform density of the satellites in the swarm cannot be obtained. Nevertheless, such a control allows to deploy more uniformly distributed swarm in the along-track direction.

Consider application of such a control using the same initial conditions of the satellites in the swarm. Set the required relative constant  $\tilde{C}_4 = 300$  m. In Fig. 17 presented the relative trajectories during 80 orbit turns and on Fig. 18 the trajectories during last two turns. Fig. 19 presents the evolution of the  $C_4$  values relative to the first launched satellite and the Fig. 20 the collision avoidance control application. From Fig. 18 and 19 one can see that the  $C_4$  values become more uniformly distributed, and since the swarm became more rarefied the dangerous rendezvous occurs less often after a time.

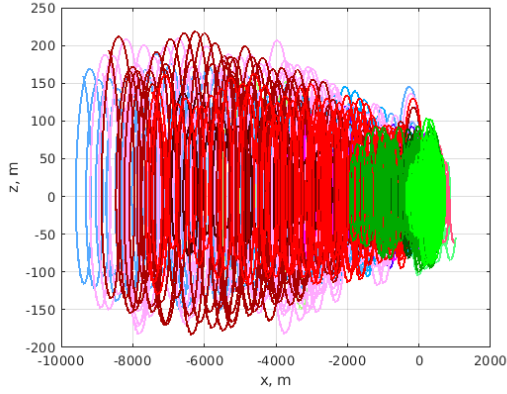


Figure 17. Relative motion trajectories

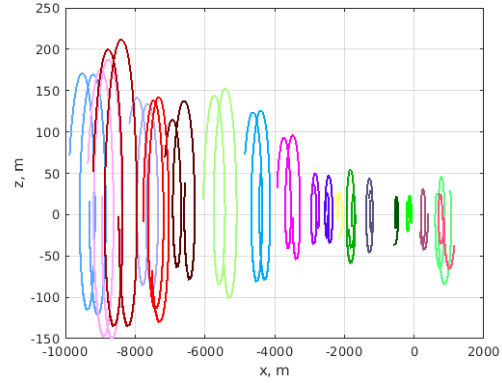


Figure 18. Relative motion trajectories during the last two turns

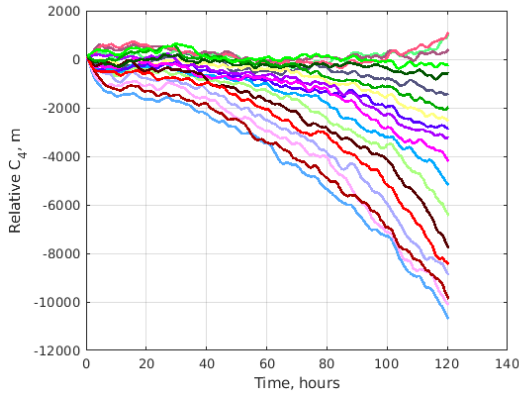


Figure 19. Values  $C_4$  relative the first launched satellite

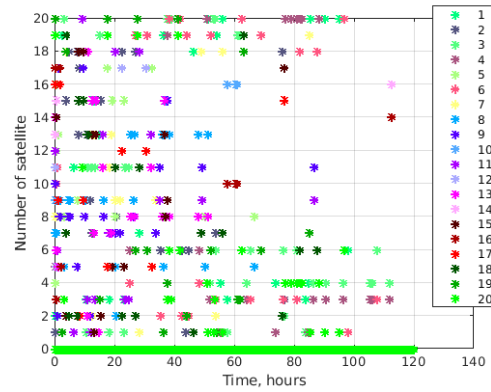
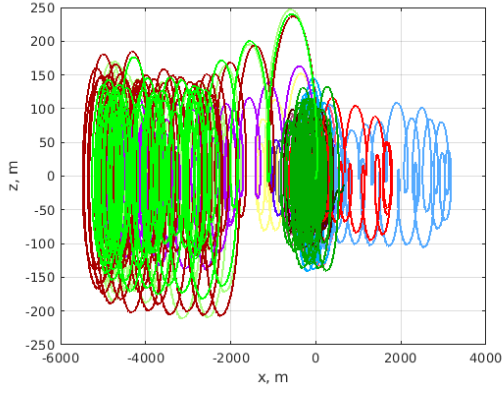


Figure 20. Collision avoidance control

## SWARM SEPARATION

The examples considered above demonstrate the successful application of the proposed rules for control in the problem of swarm control. However, the success of the swarm construction immediately after the deployment depends on a set of parameters. Consider an example of simulation when the proposed rules application lead to the decomposing of the swarm into several independent groups. This separation effect is regarded as violation of the integrity of the swarm and is considered as undesirable, though its influence may be acceptable in a certain cases.

Let all of the simulation parameters remain the same as for the previous example, except for the ejection velocity errors, that are normally distributed random values but with the same standard deviation value  $\sigma_{\delta V} = 0.015$  m/s as above. In other words, the distribution of errors remains the same, but its new specific values  $\delta V$  in (18) are taken according to the distribution. Consider the application of control rule to set to  $C_4 = 0$ , i.e. achieving the center configuration. The relative trajectories of the satellites are shown in Fig. 21 during the whole simulation time, and in Fig. 22 the trajectories during last two turns are presented. One can see that four satellites are separating from the other satellites. Fig. 23 demonstrates the values of  $C_4$  relative to the first ejected satellite and the relative  $C_4$  of the four satellites cannot converge to zero. It is caused because they fly away from the main group of satellites and after a while no other satellites enter its communicational area.



**Figure 21. Relative motion trajectories during separation**

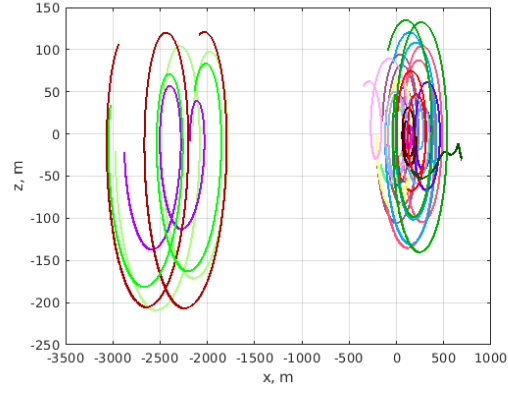


**Figure 22. Relative motion trajectories during the last two turns**

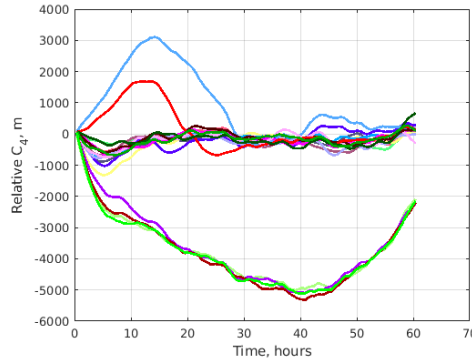


**Figure 23. Values  $C_4$  relative the first launched satellite**

The dependence of the effect of swarm separation on the parameters of the simulated launch is of particular interest and should be investigated. Since the considered ejection velocity errors are random values then the results of the swarm construction are also random. Let us investigate the performance of control rules using multiple numerical simulations with various parameters. A series of identical numerical experiments with fixed set of parameters, except for the different errors in the separation velocity but of the same normal distribution, is performed. After each simulation the relative drifts convergence to zero is checked. If the relative  $C_4$  of the set of the satellites are converged to each other but not to the  $C_4$  of the rest satellites in the swarm that satellites compose a separate group and the swarm is divided. If the swarm is divided, the number of satellites in each subgroup with the same relative drifts is calculated. Consider the number of the most numerous group of the divided swarm  $N_{group}$  as a measure of the separation effect. The effect of the swarm separation is measured using the ratio of the number of the largest subgroup to the total number of satellites in the swarm  $N_{group} / N$ . If  $N_{group} / N = 1$  it means that no satellite from the swarm is separated. If this ratio is close to 1, this corresponds to the case when a small number of satellites leave the swarm but the majority remain in the same group. If a small number of satellites flies away from the main group of the swarm it could be not a sensitive loss for the mission of the swarm. On the other hand if half of satellites lose a communication with the others it could be a significant swarm degradation.

Fig. 24 demonstrates the boxplots of the results of the numerical experiments with different size of communication area for three control strategies of the swarm – the achievement relative  $C_4 = 0$ , motion in the restricted area with  $C_4 = 500$  m and uniformly distributed swarm with

$C_4 = 300\text{ m}$  separation between the satellites – the cases of study described above. One can see that different control strategies differently affected by the communication restrictions but all of them have better performance with higher values of the communication area size.

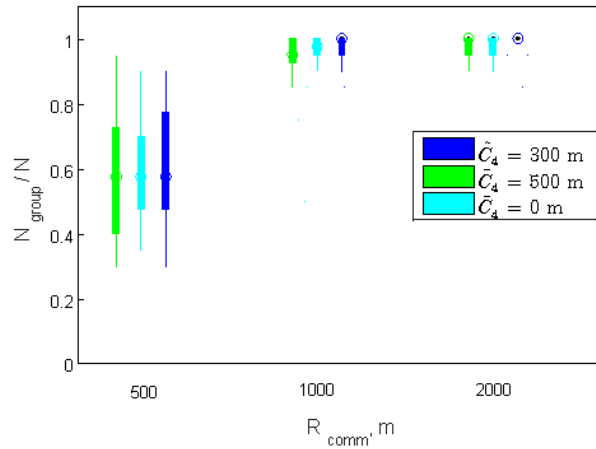


**Figure 24. Dependence of  $N_{group} / N$  on  $R_{comm}$  for different control strategies**

## CONCLUSIONS

Decentralized control based on the aerodynamic drag force allows to achieve limited motion of satellites within a given area. However, one should take into account the communication restrictions caused by the features of the relative motion determination system and inter-satellite communication. The successful use of magnetic control to implement the required attitude of the satellites relative to the incoming flow has been demonstrated. Despite the low accuracy of the stabilization of satellites with respect to the incident flow, the relative trajectories become limited. The proposed control scheme makes it possible to obtain the required limitation of the swarm of nanosatellites or to obtain uniform distribution in along track direction even in the presence of disturbances and inaccuracies in the knowledge of the density of the atmosphere.

## ACKNOWLEDGEMENTS

The work is supported by the Russian Foundation for Basic Research, grant № 17-01-00449\_a.

## REFERENCES

- <sup>1</sup> Leonard, C. L., “Formation Keeping of Spacecraft via Differential Drag,” *Master Thesis, Massachusetts Institute of Technology*, 1986.
- <sup>2</sup> Kumar, B. S., Ng, A., and Bang-Bang, A., “Control Approach to Maneuver Spacecraft in a Formation With Differential Drag,” *Proceedings of the AIAA Guidance, Navigation and Control Conference and Exhibit, AIAA Paper No.2008-6469, Honolulu, Hawaii, August 2008*.
- <sup>3</sup> Ivanov, D., Kushniruk, M., and Ovchinnikov, M., “Study of satellite formation flying control using differential lift and drag,” *Acta Astronautica*, vol. 145, Jul. 2018, pp. 88–100.
- <sup>4</sup> Pérez, D., and Bevilacqua, R., “Lyapunov-Based Adaptive Feedback for Spacecraft Planar Relative Maneuvering via Differential Drag,” *Journal of Guidance, Control, and Dynamics*, vol. 37, Sep. 2014, pp. 1678–1684.
- <sup>5</sup> Pérez, D., and Bevilacqua, R., “Differential drag spacecraft rendezvous using an

- adaptive Lyapunov control strategy,” *Acta Astronautica*, vol. 83, 2013, pp. 196–207.
- <sup>6</sup> Kumar, K. D., Misra, A. K., Varma, S., and Bellefeuille, F., “Maintenance of Satellite Formations Using Environmental Forces,” *Acta Astronautica*, vol. 102, May 2014, pp. 341–354.
- <sup>7</sup> Dellelce, L., and Kerschen, G., “Optimal propellantless rendez-vous using differential drag,” *Acta Astronautica*, vol. 109, 2015, pp. 112–123.
- <sup>8</sup> Ben-Yaacov, O., and Gurfil, P., “Long-Term Cluster Flight of Multiple Satellites Using Differential Drag,” *Journal of Guidance, Control, and Dynamics*, vol. 36, 2013, pp. 1731–1740.
- <sup>9</sup> Ben-Yaacov, O., and Gurfil, P., “Orbital elements feedback for cluster keeping using differential drag,” *Advances in the Astronautical Sciences*, vol. 153, 2015, pp. 769–787.
- <sup>10</sup> Ivanov, D., Monakhova, U., and Ovchinnikov, M., “Nanosatellites swarm deployment using decentralized differential drag-based control with communicational constraints,” *Acta Astronautica*, vol. 159, 2019, pp. 646–657.
- <sup>11</sup> Schweighart, S., and Sedwick, R. J., “High-Fidelity Linearized J2 Model for Satellite Formation Flight,” *Journal of Guidance, Control, and Dynamics*, vol. 25, 2002, pp. 1073–1080.
- <sup>12</sup> Hill, G. W., “Researches in Lunar Theory,” *American Journal of Mathematics*, vol. 1, 1878, pp. 5–26.
- <sup>13</sup> Celani, F., “Robust three-axis attitude stabilization for inertial pointing spacecraft using magnetorquers,” *Acta Astronautica*, vol. 107, Nov. 2015, pp. 87–96.
- <sup>14</sup> Ovchinnikov, M. Y., Roldugin, D. S., Ivanov, D. S., and Penkov, V. I., “Choosing control parameters for three axis magnetic stabilization in orbital frame,” *Acta Astronautica*, vol. 116, Nov. 2015, pp. 74–77.
- <sup>15</sup> Ovchinnikov, M. Y., Roldugin, D. S., and Penkov, V. I., “Three-axis active magnetic attitude control asymptotical study,” *Acta Astronautica*, vol. 110, Nov. 2015, pp. 279–286.
- <sup>16</sup> Malkin, I. G., *Some problems in the theory of nonlinear oscillations*, Oak Ridge: U.S. Atomic Energy Commission, Technical Information Service, 1959.
- <sup>17</sup> Vallado, D. A., ed., *Fundamentals of Astrodynamics and Applications*, El Segundo: Microcosm, Inc, 2001.
- <sup>18</sup> Foster, C., Mason, J., Beukelaers, V., Stepan, L., and Zimmerman, R., “Differential Drag Control Scheme for Large Constellation of Planet Satellites and On-Orbit Results,” *Proceedings of International Workshop on Satellite Constellations and Formation Flying, June 19-21, 2017. CO, Boulder, 2017*, pp. 1–18.